Insect Biochemistry and Molecular Biology 108 (2019) 24–31

Contents lists available at ScienceDirect

Insect Biochemistry and Molecular Biology

journal homepage: www.elsevier.com/locate/ibmb

DOPA decarboxylase is essential for cuticle tanning in *Rhodnius prolixus* (Hemiptera: Reduviidae), affecting ecdysis, survival and reproduction

Marcos Sterkel[a,*], Sheila Ons[a,1], Pedro L. Oliveira[b,c,1]

[a] Laboratory of Genetics and Functional Genomics, Regional Center for Genomic Studies, Faculty of Exact Sciences, National University of La Plata, Bvd 120, 1459, La Plata, 1900, Argentina

[b] Instituto de Bioquímica Médica Leopoldo de Meis, Universidade Federal do Rio de Janeiro, Av. Carlos Chagas Filho, 373, bloco D. Prédio do CCS, Ilha do Fundão, Rio de Janeiro, 21941-902, Brazil

[c] Instituto Nacional de Ciência e Tecnologia em Entomologia Molecular (INCT-EM), Rio de Janeiro, Brazil

ARTICLE INFO

Keywords:
Hematophagous arthropods
Aromatic amino acid decarboxylases
Melanin synthesis
Tyrosine metabolism

ABSTRACT

Cuticle tanning occurs in insects immediately after hatching or molting. During this process, the cuticle becomes dark and rigid due to melanin deposition and protein crosslinking. In insects, different from mammals, melanin is synthesized mainly from dopamine, which is produced from DOPA by the enzyme DOPA decarboxylase. In this work, we report that the silencing of the *RpAadc-2* gene, which encodes the putative *Rhodnius prolixus* DOPA decarboxylase enzyme, resulted in a reduction in nymph survival, with a high percentage of treated insects dying during the ecdysis process or in the expected ecdysis period. Those treated insects that could complete ecdysis presented a decrease in cuticle pigmentation and hardness after molting. In adult females, the knockdown of AADC-2 resulted in a reduction in the hatching of eggs; the nymphs that managed to hatch failed to tan the cuticle and were unable to feed. Despite the failure in cuticle tanning, knockdown of the AADC-2 did not increase the susceptibility to topically applied deltamethrin, a pyrethroid insecticide. Additionally, our results showed that the melanin synthesis pathway did not play a major role in the detoxification of the excess (potentially toxic) tyrosine from the diet, an essential trait for hematophagous arthropod survival after a blood meal.

1. Introduction

A particular characteristic of hematophagous insects is that they ingest blood quantities that represent many times their body weight in a single meal. Because the protein content represents more than 80% of the vertebrate blood dry weight, its digestion in the midgut generates amounts of free amino acids that are much larger than those observed in other organisms. Therefore, tight regulation of amino acid metabolism is particularly important in blood-sucking insects (Sterkel et al., 2017). The kissing bug *Rhodnius prolixus* is one of the vectors of *Trypanosoma cruzi*, the parasite that causes Chagas disease, which affects approximately 8 million people mainly in Central and South America, and 25 million individuals are living at risk of contracting it (World Health Organization, 2018). Recently, the *R. prolixus* genome was sequenced (Mesquita et al., 2015), generating important information for the study of enzymes involved in amino acid metabolism.

Tyrosine metabolism is especially important in insects because this amino acid is the precursor of biogenic amines and melanin. Tyrosine is necessary for the melanization of pathogens and cuticle tanning. Consequently, insect genomes encode more copies of tyrosine metabolism genes than mammals (Vavricka et al., 2014). Alternatively, tyrosine can be catabolized through a degradative pathway of five enzymatic reactions, resulting in acetoacetate and fumarate (Fig. 1A) that can be further catabolized through the Krebs cycle. In a previous report, we showed that the inhibition of any of the first two enzymes of this pathway (tyrosine aminotransferase (TAT) or 4-hydroxyphenylpyruvate dioxygenase (HPPD)) caused the death of blood-feeding arthropods after a blood meal due to the accumulation and precipitation of huge quantities of tyrosine in the hemocoel and tissues. However, the inhibition of HPPD was demonstrated to be harmless to non-hematophagous insects, revealing an essential role of this pathway in the adaptation to hematophagy by detoxifying the excess dietary tyrosine (Sterkel et al., 2016). Furthermore, the knockdown of other tyrosine metabolism enzymes drastically affects fundamental processes of *R. prolixus* physiology, such as embryogenesis, reproduction, ecdysis and nymph survival, highlighting the pleiotropic role of tyrosine

* Corresponding author.
E-mail addresses: msterkel@conicet.gov.ar (M. Sterkel), sheila.ons@presi.unlp.edu.ar (S. Ons), pedro@bioqmed.ufrj.br (P.L. Oliveira).
[1] Both authors contributed equally to this manuscript.

https://doi.org/10.1016/j.ibmb.2019.03.006
Received 5 December 2018; Received in revised form 25 February 2019; Accepted 12 March 2019
Available online 15 March 2019
0965-1748/

Abbreviations

AADCs	aromatic amino acids decarboxylases enzymes
TAT	tyrosine aminotransferase
HPPD	4-hydroxyphenylpyruvate dioxygenase
DDC	DOPA decarboxylase
TH	tyrosine hydroxylase
NBAD	N-β-alanyldopamine
NADA	N-acetyldopamine
PO	phenoloxidase
DCE	dopachrome conversion enzyme
DCT	dopachrome tautomerase
DOPA	L-3,4-dihydroxyphenylalanine
TD	tyrosine decarboxylase
PBS	phosphate-buffered saline
dsRNA	double-stranded RNA
RNAi	RNA interference
QPCR	quantitative polymerase chain reaction
PBM	post-blood meal
cDNA	complementary DNA
HD	histidine decarboxylase
N1	first instar nymphs
N4	fourth instar nymphs
MAL	maltose-binding protein
LD50	lethal dose that kills 50% of treated insects

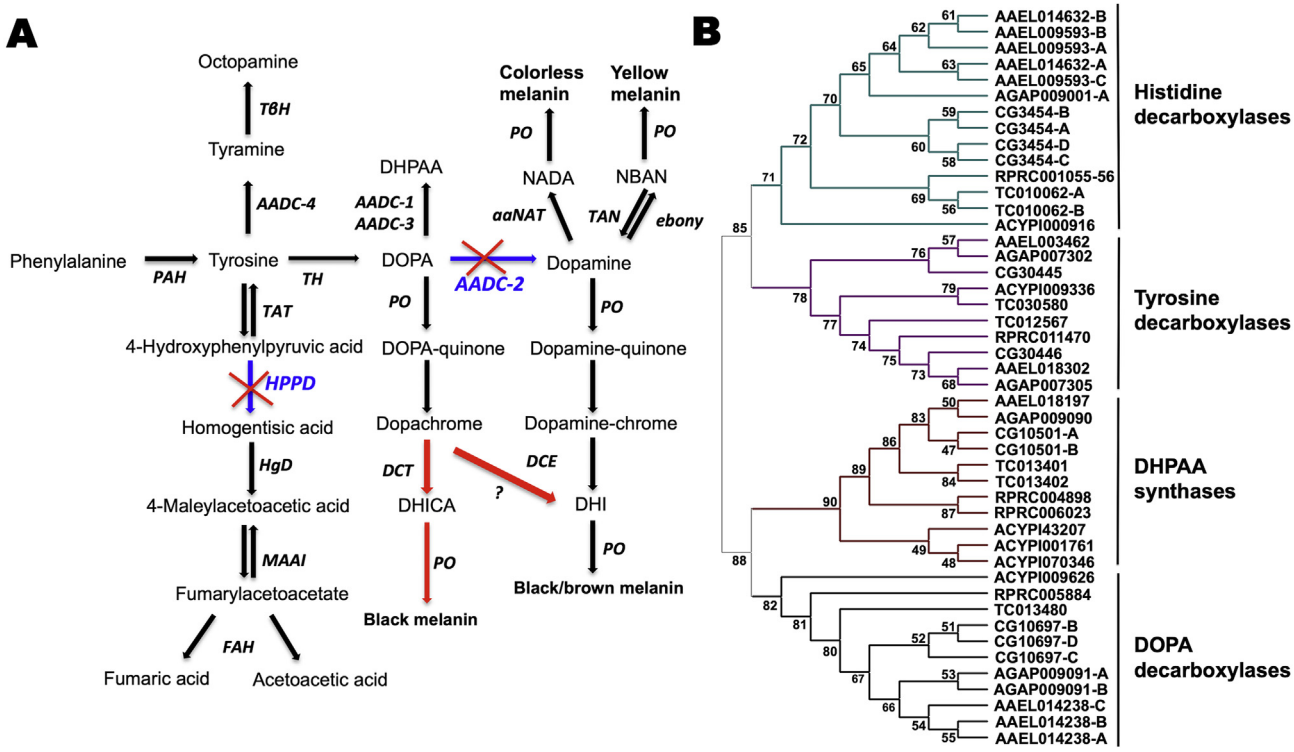

Fig. 1. A: Tyrosine metabolism pathways in *R. prolixus*. PAH: phenylalanine hydroxylase; TAT: tyrosine aminotransferase; HPPD: 4-hydroxyphenylpyruvate dioxygenase; HgD: homogentisate 1,2-dioxygenase; MAAI: maleylacetoacetate isomerase; FAH: fumarylacetoacetase; TH: tyrosine hydroxylase, AADC: aromatic L-amino acid decarboxylase; PO: phenoloxidase; DCE: dopachrome conversion enzyme, DCT: dopachrome tautomerase (not described in insects) aaNAT: aralkylamine N-acetyltransferase; TβH: tyramine β-hydroxylase. The metabolites are abbreviated as follows: L-DOPA: L-3,4-dihydroxyphenylalanine; DHI: 5,6-dihydroxyindole, NADA: N-acetyldopamine; NBAN: N-β-alanyldopamine. Red arrows describe possible pathways that are not described in insects. B: Aromatic L-amino acid decarboxylases phylogenetic analysis. Note that AADC-2 (RPRC005848) is grouped with DOPA decarboxylases, AADC-1 and AADC-3 (RPRC004898 and RPRC006023) are grouped with DHPAA synthases, and AADC-4 is grouped with tyrosine decarboxylase enzymes from other insects. RPRC: *Rhodnius prolixus*. TC: *Tribolium castaneum*. ACYPI: *Acyrthosiphon pisum*. AAEL: *Aedes aegypti*. AGAP: *Anopheles gambiae*. CG: *Drosophila melanogaster*. (For interpretation of the references to color in this figure legend, the reader is referred to the Web version of this article.)

catabolism enzymes in this insect (Sterkel and Oliveira, 2017).

In the melanin synthesis pathway, DOPA and dopamine are synthesized from tyrosine by tyrosine hydroxylase (TH) and DOPA decarboxylase (DDC) enzymes, respectively. Dopamine, in turn, can be converted into two other major catecholamine metabolites, N-β-alanyldopamine (NBAD) and N-acetyldopamine (NADA). Finally, the melanin required for pigmentation is produced from these catecholamines by phenoloxidases (POs) that change these products to their respective quinones, which are then converted to DOPA melanin (black pigment), dopamine melanin (brown/black), NBAD melanin (yellow), or NADA melanin (colorless) (Borowsky et al., 2001; Wittkopp and Beldade, 2009) (Fig. 1A). Moreover, oxidative conjugation of these quinones to cuticular proteins is necessary for the crosslinking of adjacent polypeptide chains, a process necessary for sclerotization (Mun et al., 2015; Riedel et al., 2011). Different from mammals, in which melanin is synthetized from DOPA, in all the insect species studied to date, most of them holometabolous, melanin is synthetized mainly from dopamine (Barek et al., 2018; Hiruma and Riddiford, 1984; Hiruma et al., 1985; Liu et al., 2014). Thus, the correct function of DDC is crucial for those physiological processes that require melanin (Arakane et al., 2009; Davis et al., 2008; Futahashi and Fujiwara, 2005; Huang et al., 2005; Macey et al., 2005; Nappi et al., 1992; Paskewitz and Andreev, 2008; Sideri, et al., 2008). Additionally, dopamine is a neurotransmitter (Verlinden, 2018). Members of the aromatic amino acid decarboxylase (AADC) family are also involved in the synthesis of other neurotransmitters, such as tyramine, octopamine (also derived

from tyrosine; Fig. 1A) and serotonin (derived from tryptophan). These amines selectively activate G-protein-coupled receptors to exert their biological function (Balfanz et al., 2014; Bunzow et al., 2001; Wragg et al., 2007).

The *Drosophila melanogaster* genome encodes four AADCs: a typical DOPA decarboxylase (dDDC; gene number CG10697), two tyrosine decarboxylases (dTD1 and dTD2; gene numbers CG30445 and CG30446), and one α-methyl-DOPA-resistant protein (dAMD, gene number CG10501) (Han et al., 2010). Recently, it was demonstrated that α-methyl-DOPA-resistant proteins use L-DOPA as a substrate, as does DDC, but they catalyze the production of 3,4-dihydroxylphenylacetaldehyde (DHPAA). Hence, the authors proposed to rename this enzyme DHPAA synthase (Vavricka et al., 2011). In *Drosophila*, the *Ddc* gene expression pattern is complex and varies among different developmental stages and innate immune responses (Davis et al., 2007, 2008). In this insect, dDdc mRNAs are alternatively spliced to produce epidermal or neural-specific transcripts (Morgan et al., 1986). This enzyme was demonstrated to be active toward L-DOPA and 5-hydroxytryptophan but had no activity toward tyrosine, D-DOPA or tryptophan (Han et al., 2010). *D. melanogaster Ddc*-null mutants are homozygous lethal. Using transgenes to supply the epidermal isoform, but not the neural-specific isoform, the lethal phenotype was rescued (Morgan et al., 1986). DDC also affects *D. melanogaster* longevity (De Luca et al., 2003). In the mosquito *Anopheles gambiae,* silencing of the *Ddc* or *Dopachrome conversion enzyme* (*Dce*) genes reduces melanization during the immune response (Paskewitz and Andreev, 2008). *Ddc*-silenced *Aedes aegypti* also presented reduced melanization of inoculated microfilariae. These mosquitoes exhibit high mortality, over-feeding and abnormal movement, consistent with an involvement of DDC in neurotransmission (Huang et al., 2005).

In *D. melanogaster,* DHPAA synthase is expressed in tissues that produce cuticle materials. Apparent defects in regions of colorless, flexible cuticular structures have been observed in DHPAA synthase mutants (Vavricka et al., 2011). DHPAA is highly toxic because its aldehyde group reacts with the primary amino groups of proteins, leading to protein crosslinking and inactivation. Hence, DHPAA synthases were proposed to be involved in the formation of flexible cuticle through their reactive DHPAA-mediated protein crosslinking reactions (Vavricka et al., 2011). By contrast, tyrosine decarboxylase (TD) enzymes are expressed in nervous tissue. *D. melanogaster Td2*-mutants lack neural tyramine and octopamine and are female sterile due to egg retention (Cole et al., 2005).

The *R. prolixus* genome encodes four putative AADCs enzymes, each presenting a particular tissue expression pattern (Figs. 1 and S1). In a previous work, we reported that the chemical inhibition of AADCs by carbidopa in female *R. prolixus* resulted in a delay in oviposition and a small reduction in the egg-hatching rate (Sterkel and Oliveira, 2017). Given that melanin synthesis is a major tyrosine-consuming pathway and tyrosine detoxification is essential for hematophagous insect survival after a blood meal, in the present work we evaluated the relevance of AADC-*2*, the putative DOPA decarboxylase enzyme, in the physiology of *R. prolixus* using RNA interference (RNAi).

2. Materials and methods

2.1. Ethics statement

All the animal work was conducted according to the guidelines of the institutional care and use committee (Committee for Evaluation of Animal Use for Research from the Federal University of Rio de Janeiro), which is based on the National Institutes of Health Guide for the Care and Use of Laboratory Animals (ISBN 0-309-05377-3). The protocols received registry number 115/13 from the Animal Ethics Committee (Comissão de Ética no Uso de Animais, CEUA). Technicians at the animal facility at the Institute of Medical Biochemistry (UFRJ) performed all aspects related to rabbit husbandry under strict guidelines to ensure careful and consistent handling of the animals.

2.2. Rearing of insects

R. prolixus were maintained under a photoperiod of 12 h of light/darkness, at 28 °C and 50-60% relative humidity. The insects were fed on rabbits at 4-week intervals. Only mated adult females that had been previously fed once during the adult stage were used to perform the experiments.

2.3. AADC phylogenetic analysis

The phylogenetic (Fig. 1B) analyses were conducted using MEGA 7 software (Kumar et al., 2016). The evolutionary history was inferred using the maximum likelihood method based on the JTT matrix-based model (Jones et al., 1992). The tree with the highest log likelihood (−4904.31) is shown. Initial tree(s) for the heuristic search were obtained automatically by applying Neighbor-Join and BioNJ algorithms to a matrix of pairwise distances estimated using a JTT model, and then selecting the topology with a superior log likelihood value. The analysis involved 46 amino acid sequences.

2.4. RNA isolation and cDNA synthesis

R. prolixus tissues were dissected in ice-cold PBS (0.15 M NaCl, 10 mM Na-phosphate, pH 7.4). The total RNA from different tissues was extracted using TRIzol reagent (Invitrogen, San Diego, CA, USA) according to the manufacturer's instructions. Following treatment with DNase (Fermentas International Inc., Burlington, Canada), first-strand cDNA synthesis was performed using 1 μg of total RNA with the "Superscript III First-strand Synthesis System for RT-PCR Kit" (Applied Biosystems, Foster City, CA) and random hexamers according to the manufacturer's instructions.

2.5. Synthesis of double-stranded RNA (dsRNA)

Specific primers for *RpAadc-2* genes were designed. The same primers previously used for amplification of the *RpHppd* gene by PCR were used in this work (Sterkel and Oliveira, 2017; Sterkel et al., 2016). These primers contained the T7 polymerase binding sequence at the 5′ end, required for dsRNA synthesis (Table 1). The *maltose-binding protein* (*Mal*) gene from *Escherichia coli* (GenBank: KIH35983.1) was used as a control for the off-target effects of dsRNA injection. It was amplified

Table 1
Sequences of the primers used to amplify target genes for RNAi experiments. T7 promoter sequences that were necessary for transcription are shown in red. All sequences and accession numbers used are as found in the Vectorbase database (https://www.vectorbase.org/).

Gene	Vector Base ID	Forward primer	Reverse primer
Aadc-2	RPRC005884	TAATACGACTCACTATAGGGA GACTGAGACCGCTCATCCCATC	TAATACGACTCACTATAGGGA GAGCCACTAGGGTTGCTTCACT
Hppd	RPRC003878	TAATACGACTCACTATAGGGA GAAGTGCAGCCAAATGGTACGA	TAATACGACTCACTATAGGGA GAAGAACAGAGTGGGTCGGTCT

from the Litmus 28i-mal plasmid (New England Biolabs) using T7 promoter primers. The PCR products were sequenced to identity confirmation. Double-stranded RNAs were synthesized using the MEGAscript RNAi kit (Ambion) according to the manufacturer's instructions. The dsRNA concentrations were determined spectrophotometrically using the Nanodrop 1000 spectrophotometer v.3.7 (Thermo Fisher Scientific) and were visualized in an agarose gel (1.5% w/v) to verify the dsRNA size, integrity and purity.

2.6. RNAi to determine loss-of-function phenotypes

Fourth instar nymphs (N4) and adult female *R. prolixus* were injected in the thorax with 2.5 μg of each target gene dsRNA dissolved in 1 μl of ultrapure water using a 10-μl Hamilton microsyringe. Control insects were injected with 2.5 μg of Mal dsRNA. Insects were fed on rabbits 7 days after dsRNA injection, which was considered day 0. On that day, some starved insects were dissected, and tissues were collected in Trizol reagent (Invitrogen, San Diego, CA, USA) to check the efficacy of gene knockdown by QPCR. First instar nymphs (N1) were collected 7 days after hatching from eggs laid by dsMal (Control) or dsAadc-2 treated females.

2.7. Quantitative polymerase chain reaction (QPCR)

Total RNA was extracted from the intestine (anterior midgut, posterior midgut and rectum) in the case of females and N4 or from the whole body in the case of N1. cDNA was synthesized as previously described. Specific primers for each target gene were designed to amplify a different region from that amplified by the RNAi primers to prevent dsRNA amplification that may be retrotranscribed during the synthesis of the cDNA together with insect RNA. They were also designed in different exons to prevent genomic DNA amplification, and their efficiency was experimentally tested (Table 2). The 18S genes were used as reference (housekeeping) genes (Majerowicz et al., 2011; Paim et al., 2012). QPCR was performed using the Brilliant III Ultra-Fast SYBR® Green QPCR Master mix (Applied Biosystems) under the following conditions: 95 °C for 15 min, followed by 40 cycles of 95 °C for 15 s, 60 °C for 30 s and 72 °C for 30 s and a final cycle of 72 °C for 10 min. The $2e^{-\Delta CT}$ values obtained for dsAadc-2- and dsMal-injected insects were used to evaluate the gene-silencing efficacy (Livak and Schmittgen, 2001). T-test was used to evaluate significant differences between the experimental and control groups.

2.8. Survival experiments

Insect survival was scored daily during 164 days after the blood meal (PBM), considered as day 0 PBM. The log-rank (Kaplan-Meier) test was used to evaluate significant differences in survival between the experimental and control groups.

2.9. Oviposition and eclosion

Fully engorged females were individually separated into vials and kept at 28 °C and 50–60% relative humidity, under a photoperiod of 12 h of light/12 h of darkness. The number of eggs laid by each female was counted daily. The eclosion ratios were calculated by dividing the number of hatched first-instar nymphs by the number of eggs laid by each female. Two-way ANOVA was used to evaluate significant differences between the experimental and control groups.

2.10. Topical application of deltamethrin

Topical applications of 0.2 μl of five serial deltamethrin dilutions (0.5–0.003125 ng/μl; 1 to 0.00625 μM) in acetone were applied in the abdomen of first-instar nymphs (N1) with the aid of a 10-μl Hamilton microsyringe equipped with a dispenser. At least 10 starved N1 hatched from eggs laid by dsMal or dsAadc-2 treated females (approximately 10 days old) were used per dose and per replicate. Control groups received 0.2 μl of acetone. After treatment, N1 were kept as described above, and the mortality was recorded every 24 h for 3 days. Probit analysis (POLO Plus version 2.0) was performed to evaluate differences between controls (MAL) and *RpAadc-2*-silenced N1 in the susceptibility to deltamethrin.

2.11. Statistical analysis

At least three independent experiments were performed for each treatment, each with N = 8–15 insects per experimental group. The data from multiple experiments were combined into a single graph. Statistical analysis and design of the graphs were performed using Prism 6.0 software (GraphPad Software, San Diego, CA).

3. Results and discussion

3.1. AADC identification and expression pattern in R. prolixus

Searches in the *R. prolixus* genomic database (www.vectorbase.org) revealed that it expresses four putative AADCs enzymes. Phylogenetic analysis (Fig. 1B) indicated that one of them (RpAADC-2; RPRC005884) is closely related to DOPA decarboxylases from other insects, two (RpAADC-1 and RpAADC-3; RPRC004898 and RPRC006023) are more similar to DHPAA synthase enzymes, and one (RpAADC-4; RPRC011470) presents characteristic features of a tyrosine decarboxylase enzyme. No alternative splicing forms were found for these genes in *R. prolixus*. Another sequence presented similarity to AADCs, but phylogenetic analysis placed this gene product in the histidine decarboxylases branch (HD) (Fig. 1B). AADCs and HDs both belong to group II decarboxylase enzymes; they share many structural and functional features and are characterized by the presence of a pyridoxal-dependent decarboxylase conserved domain (Sanchez-Jimenez et al., 2016).

Transcriptomic data analysis of published *R. prolixus* cDNA libraries (Ribeiro et al., 2014) indicate that the *RpAadc-1* gene, coding for a putative DHPAA synthase, is expressed in the digestive system, mainly in the rectum (hindgut) but also in the anterior and posterior midgut (Fig. S1A). The rectum of insects is derived from ectodermal cells; it produces a cuticle and undergoes ecdysis (Rowland and Goodman, 2016). Attachment of *T. cruzi* to the rectal cuticle of triatomines is

Table 2
Sequence of the primers used to quantify target genes by QPCR. The primer efficiencies were experimentally verified for each pair of primers. All sequences and accession numbers used were as found in the Vectorbase database (https://www.vectorbase.org/), except the Ribosomal protein 18S, which was present in version 1.0 of the *Rhodnius* genome and was removed from VectorBase in the RproC3 assembly. The *R. prolixus* 18S rRNA gene can be found in the NCBI database with the accession number indicated below.

Gene	Vector Base/NCBI ID	Forward primer	Reverse primer	% Efficiency
Ribosomal rRNA 18S	AJ421962	TGTCGGTGTAACTGGCATGT	TCGGCCAACAAAAGTACACA	89.2
Aadc-2	RPRC005884	TCCTTCGTGGGTTGTGAACG	GTGCACGAAATCGCCTACCT	83.5
Hppd	RPRC003878	GCTAAACAGGCGGCCAGCTA	TGGACGCTCTGTAACCAGGA	98.6

essential for parasite development and metacyclogenesis and involves adhesion to hydrophobic components of the cuticle surface (Azambuja et al., 2005; Schaub et al., 1998). The expression of *RpAadc-1* in the *R. prolixus* rectum is an interesting finding; further studies are required to address its function.

Among the four members of the AADC family, *RpAadc-2*, the putative *DOPA decarboxylase* gene, presented the highest expression in whole-body samples (Fig. S1B), but its expression in several tissues analyzed was low (anterior midgut, posterior midgut, rectum, fat body, Malpighian tubules, ovaries and testis). The former indicated that it could be mainly expressed in other tissues that were not sequenced, such as cuticle epithelium, hemocytes, nervous system and/or flight muscle (Fig. S1B). Accordingly, the orthologous enzyme in *D. melanogaster* is mainly expressed in the epidermis and is also expressed in the brain (Morgan et al., 1986).

The *RpAadc-3* gene, which encodes the other putative DHPAA synthase enzyme, presented a low number of reads in whole-body libraries, and its transcription was not detected in any of the tissues that were analyzed (Fig. S1C). The expression of the *RpAadc-4* gene, encoding the tyrosine decarboxylase enzyme (TD) that uses tyrosine as a substrate to produce tyramine, was not detected in any of the tissues sequenced or in whole-body samples, indicating that its expression is low. Phylogenetic analysis indicated that this enzyme is closely related to *D. melanogaster* TD-2 (CG30446, Fig. 1B), which is expressed in nervous tissue.

Due to the importance of tyrosine metabolism in insects in general, particularly in hematophagous arthropods (Sterkel et al., 2017; Vavricka et al., 2011), in this work we focused on AADC-2, the putative *R. prolixus* DOPA decarboxylase enzyme, which presents the highest expression level among AADCs (Fig. S1). To study its physiological relevance, RNAi-mediated gene silencing was used in fourth-instar nymphs (N4) and adult females. Because this enzyme is part of a major tyrosine-consuming pathway, we hypothesized that it could be important in the detoxification of excess tyrosine from the diet of hematophagous insects, as was previously observed for TAT and HPPD (Sterkel et al., 2016). We also performed experiments where the *RpAadc-2* and *RpHppd* genes were silenced together (HPPD/AADC-2 group). In all cases, a significant level of gene silencing was achieved (Fig. S2).

3.2. *RpAadc-2* functional analysis in nymphs and adult females through gene silencing

Of the 47 dsAadc-2-injected *R. prolixus* N4 individuals, only 23 successfully molted to fifth-instar nymphs (N5. Fig. 2A–C) and the N5 emerged nymphs lacked the typical black pigmentation in the cuticle (Fig. 2D and E). Moreover, when probed with tweezers, they clearly showed a softer exoskeleton than controls. Of the 24 nymphs that did not molt successfully, 13 insects died during ecdysis (aborted ecdysis phenotype), and the remaining 11 died as N4, most of them during the expected ecdysis period (Fig. 2A–C). The aborted ecdysis phenotype has been previously described in *R. prolixus* for the knockdown of tyrosine hydroxylase (TH), the first enzyme in the melanin synthesis pathway (Sterkel and Oliveira, 2017). However, different from AADC-2 knockdown, all the nymphs injected with dsTh presented the aborted ecdysis phenotype (Sterkel and Oliveira, 2017). When the *Aadc*-2-silenced N4 that failed to complete ecdysis were manually dissected, they presented a new untanned cuticle but failed to get out of the old cuticle.

The survival of the emerged untanned N5 was reduced compared with that of the control group (Fig. 2A and B $p < 0.0001$). Despite the high mortality observed in *Aadc-2*-silenced insects, different from the HPPD-knockdown phenotype, no accumulation of tyrosine crystals in the hemocoel was observed. This fact suggested that the higher rate of death was not due to tyrosine accumulation and precipitation but was instead due to failure in cuticle tanning (Fig. 2A–C). Most control insects (dsMal; 32 of 37) normally molted to N5 at the expected ecdysis time. Altogether, the results revealed that dopamine-melanin, not DOPA-melanin, is the predominant pigment in *R. prolixus,* as has been described for other insects (Barek et al., 2018; Hiruma and Riddiford, 1984; Hiruma et al., 1985; Liu et al., 2014). The failure in AADC-2 function prevented cuticle tanning, and this process is essential for ecdysis and the survival of nymphs.

To gain more extensive knowledge about the role of AADC-2 in *R. prolixus*, we also performed RNAi experiments in adult females. In these insects, the knockdown of AADC-2 was not lethal after a blood meal (Fig. 3A), confirming the previous conclusion that the reduced survival observed in nymphs was not due to tyrosine accumulation but failure in cuticle tanning. Although it did not affect female survival, AADC-2 knockdown caused a delay in oviposition (Fig. 3B) and a reduction in the hatching of eggs (Fig. 3C). Similar to the TH knockdown phenotype (Sterkel and Oliveira, 2017), in the eggs laid by *Aadc-2*-silenced

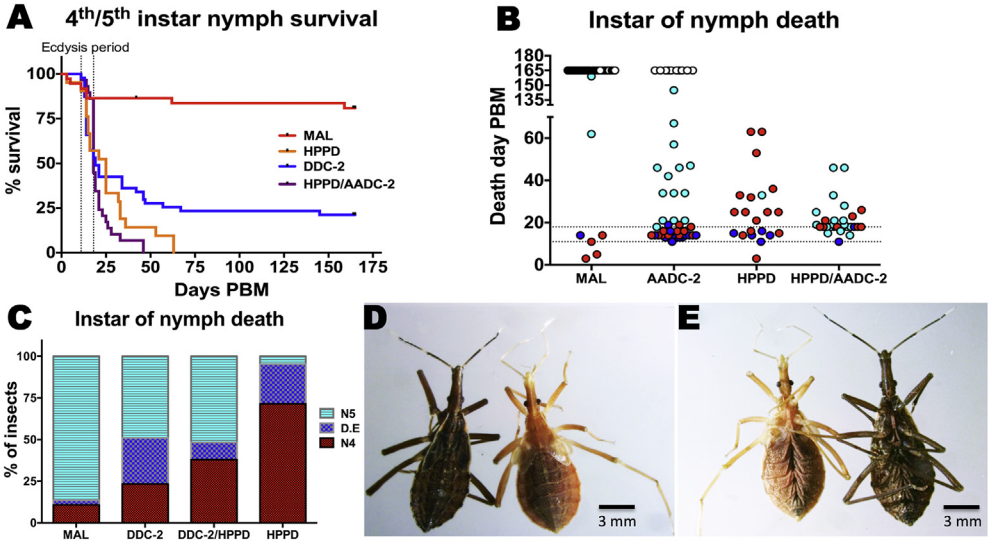

Fig. 2. AADC-2 activity is essential for cuticle tanning after ecdysis in *R. prolixus*. A: Survival of dsRNA-injected fourth-instar nymphs (N4) after a blood meal (PBM). The dotted vertical lines show the ecdysis period. Insect survival was recorded until 164 days PBM. B: Instar of death of insects. Red dots represent insects that died as N4. Blue dots represent insects that died during the ecdysis process, cyan dots represent insects that died as fifth-instar nymphs (N5), and white dots represent N5 that survived longer than 164 days. The dotted lines show the ecdysis period. C: Instar of insect's death shown as a percentage. In all cases, at least two independent experiments were performed, each with N = 8–15 insects per experimental group. The data from multiple experiments were combined into a single graph. D: Dorsal view of control (left) and *RpAadc-2*-silenced (right) insects. E: Ventral view of *RpAadc-2*-silenced (left) and control (right) insects. (For interpretation of the references to color in this figure legend, the reader is referred to the Web version of this article.)

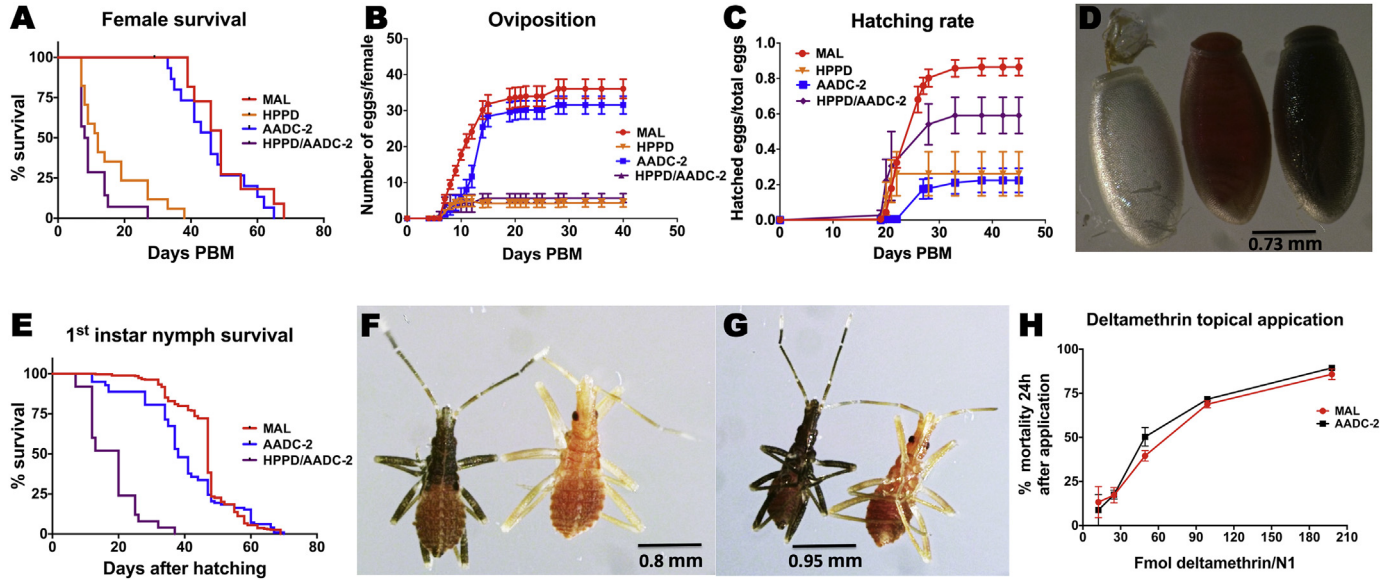

Fig. 3. AADC-2 activity is required for reproduction. A: *R. prolixus* female survival after AADC-2 and/or HPPD knockdown by dsRNA injection. B: Number of eggs laid. C: Hatching rate of egg. D: Phenotype of the eggs laid by control (left), *RpHppd*-silenced (center) and *RpAadc-2*-silenced females (right). Images were taken 20-21 days after the eggs were laid. F: Dorsal view of first-instar nymphs (N1) hatched from eggs laid by dsMal-injected (left) or with dsAadc-2-injected females (right). E: Survival of first-instar nymphs. G: Ventral view of N1 (left) hatched from eggs laid by dsMal-injected (left) or ds dsAadc-2-injected females (right). H: Susceptibility of control (MAL) and *RpAadc-2*-silencd N1 to deltamethrin. The data were plotted as the mean ± s.e.m in panels B, C and H. For all panels, at least two independent experiments were performed, each with N = 8–15 insects per experimental group. The data from multiple experiments were combined into a single graph.

females, embryo development proceeded until a late stage of embryogenesis with first-instar nymphs fully developed (Fig. 3C), but only approximately 20% could hatch (Fig. 3D). However, different from TH knockdown, in which the nymphs that managed to hatch presented a normal phenotype (Sterkel and Oliveira, 2017), the nymphs that hatched from eggs laid by dsAadc-2-injected females failed to tan the cuticle, as observed in N5 after ecdysis, but their survival was not significantly reduced (Fig. 3F and G). These nymphs could not feed because they could not bite the skin of the rabbit host, probably due to failure in sclerotization of mouthparts. These results further confirmed that melanin in *R. prolixus* is synthetized from dopamine and not from DOPA as in mammals (Barek et al., 2018).

Contact insecticides must penetrate through the cuticle to reach their action sites; impairments in cuticle penetration are involved in insecticide resistance in several species (Balabanidou et al., 2018), including the kissing bug *Triatoma infestans* (Pedrini et al., 2009). Because *Aadc-2*-silenced insects failed to tan the cuticle, we hypothesized that they might be more susceptible to topical application of insecticides. Quite unexpectedly, no significant differences were observed in the susceptibility to deltamethrin between control and *Aadc-2*-silenced N1, presenting a LD50 (95% confidence interval) equal to 79.44 (58.26–102.37) and 64. 93 fmol/nymph (46.72–88.39), respectively (0.040 and 0.033 ng of deltamethrin per nymph. Fig. 3H). These results revealed that AADC-2 knockdown did not increase susceptibility to deltamethrin as might be expected due to the failure in cuticle tanning.

3.3. *RpAadc-2* gene silencing in conjunction with *RpHppd* gene silencing. Functional analysis in nymphs and adult females

In this work we repeated HPPD knockdown to allow direct comparison with the *Hppd/Aadc-2* double-silenced group. As was observed in our previous works (Sterkel and Oliveira, 2017; Sterkel et al., 2016), the knockdown of HPPD was lethal after a blood meal due to tyrosine accumulation, leading to the precipitation of tyrosine crystals in hemocoel and tissues. Of 21 dsHppd-injected N4, only 1 molted to N5, 5 died during ecdysis and 15 died as N4, notwithstanding 11 of them survived much longer than the expected ecdysis period (Fig. 2A–C). The *Hppd/Aadc-2* double-silenced insects presented the same lethal phenotype associated with tyrosine accumulation and precipitation observed in *Hppd*-silenced insects. However, different from the HPPD phenotype, around one-half of N4 performed ecdysis ($p < 0.05$) and the N5 presented the pale phenotype associated with AADC-2 knockdown (Fig. 2A–C). Of 29 dsHppd/Aadc-2 injected N4, 15 molted into N5, while 11 died as N4 and 3 during the ecdysis process (Fig. 2A–C). These untanned N5 also presented tyrosine crystals in hemocoel and tissues, as observed in *Hppd*-silenced nymphs, indicating superposition of both phenotypes. The rate of death was enhanced in the *Hppd* and *Hppd/Aadc-2*-silenced groups compared with that in *Aadc-2*-silenced insects (Fig. 2A and B).

Most of the females injected with Hppd and Hppd/Aadc-2 dsRNA died at the onset of oogenesis (Fig. 3A), so they laid only a few eggs (Fig. 3B). Most of the eggs laid by *Hppd*-silenced females did not develop into embryos, and the hatching rate was approximately 20% (Fig. 3C and D). Because of the combined effect of a reduced number of eggs laid and their reduced hatching, the reproductive fitness of dsHppd-injected females was drastically reduced. Unexpectedly, the phenotype associated with a reduced hatching rate observed in *Hppd*- and *Aadc-2*-silenced insects was partially reverted in *Hppd/Aadc-2* double silenced animals. In this group, in contrast to the dsHppd and dsAadc-2 phenotypes ($p < 0.005$), approximately 60% of nymphs hatched and they also failed to tan the cuticle, as observed for AADC-2 knockdown (Fig. 3C). In contrast to *Aadc-2*-silenced N1, *Hppd/Aadc-2*-silenced N1 presented a reduced survival compared with controls although they were not fed on blood (Fig. 3E, $p < 0.0001$).

A similar survival rate was observed in the *Hppd*- and *Hppd/Aadc-2*-silenced groups in N4 and females ($p = 0.1686$ and $p = 0.081$, respectively. Figs. 2A and 3A), suggesting that the double silencing of *Hppd/Aadc-2* genes was not additive regarding the lethal effect of H*ppd* silencing. These results, in concordance with those previously obtained for *Hppd/Th* and *Hppd/Po* double-silenced insects (Sterkel et al., 2016), indicate that the melanin synthesis pathway does not play a major role in tyrosine detoxification.

In *Hppd*-silenced insects, melanin deposition was observed around tyrosine crystals (Sterkel et al., 2016), suggesting that excess melanin

synthesis (that produce highly reactive o-quinones intermediates and reactive oxygen species (ROS); reviewed by (Vavricka et al., 2014)) might be involved in the extensive tissue damage observed and death of insects. Nevertheless, this phenotype was not reverted by the knockdown of phenoloxidases or tyrosine hydroxylase enzyme (Sterkel et al., 2016). The knockdown of AADC-2, the enzyme that supplies the dopamine necessary for melanin synthesis, also failed to rescue the lethal phenotype observed upon *Hppd*-silencing, further confirming the hypothesis that melanin formation around tyrosine crystals is not required for the lethal phenotype to occur. Interestingly, in *Hppd/Aadc-2* double-silenced insects, some HPPD-associated phenotypes, such as no ecdysis in N4 and reduced hatching of the eggs, were partially rescued. Further studies are required to address the reasons for the partial reversion of these phenotypes.

To summarize, in this work we found that the correct function of AADC-2, the DOPA decarboxylase enzyme, is essential for cuticle tanning. Thus, melanin is synthetized mainly from dopamine in *R. prolixus*. The failure in cuticle tanning affected essential processes of *R. prolixus* physiology, such as ecdysis, survival and hatching. It also prevented feeding because insects could not pierce the skin of the rabbit hosts. However, quite unexpectedly, failure in cuticle tanning did not increase the susceptibility of nymphs to topically applied deltamethrin. Altogether, these results indicate that the melanin synthesis pathway is conserved among the class *Insecta* and do not present any particular phenotype related to hematophagy as observed for other enzymes involved in tyrosine metabolism. These results further highlight the unique importance of the TAT/HPPD catabolism pathway in the detoxification of excess dietary tyrosine in blood-sucking insects and, consequently, in the adaptation to hematophagy.

Funding

This work was supported by FAPERJ (Brazil), CNPq (Brazil) and ANPCyT (Argentina), even though this research, in particular, did not receive any specific grant. Funders did not have any role in study design; in the collection, analysis and interpretation of data; in the writing of the report; and in the decision to submit the article for publication.

Declarations of interest

None.

Acknowledgements

We would like to thank Charlion Cosme, José de S. Lima, Jr., and Gustavo Ali for their technical assistance. We also thank Dr. Gonzalo Roca Acevedo for helping us with the analysis of the data from deltamethrin topical application assays.

Appendix A. Supplementary data

Supplementary data to this article can be found online at https://doi.org/10.1016/j.ibmb.2019.03.006.

References

Arakane, Y., Lomakin, J., Beeman, R.W., Muthukrishnan, S., Gehrke, S.H., Kanost, M.R., Kramer, K.J., 2009. Molecular and functional analyses of amino acid decarboxylases involved in cuticle tanning in Tribolium castaneum. J. Biol. Chem. 12 (24), 16584–16594. https://doi.org/10.1074/jbc.M901629200. 284.

Azambuja, P., Ratcliffe, N.A., Garcia, E.S., 2005. Towards an understanding of the interactions of *Trypanosoma cruzi* and *Trypanosoma rangeli* within the reduviid insect host *Rhodnius prolixus*. An. Acad. Bras. Cienc. 77, 397–404. https://doi.org//s0001-37652005000300004.

Balabanidou, V., Grigoraki, L., Vontas, J., 2018. Insect cuticle: a critical determinant of insecticide resistance. Curr Opin Insect Sci. 27, 68–74. https://doi.org/10.1016/j.cois.2018.03.001. Jun.

Balfanz, S., Jordan, N., Langenstuck, T., Breuer, J., Bergmeier, V., Baumann, A., 2014. Molecular, pharmacological, and signaling properties of octopamine receptors from honeybee (*Apis mellifera*) brain. J. Neurochem. 129, 284–296. https://doi.org/10.1111/jnc.12619.

Barek, H., Sugumaran, M., Ito, S., Wakamatsu, K., 2018. Insect cuticular melanins are distinctly different from those of *Mammalian* epidermal melanins. Pigment Cell Melanoma Res 31, 384–392. https://doi.org/10.1111/pcmr.12672.

Borowsky, B., Adham, N., Jones, K.A., Raddatz, R., Artymyshyn, R., Ogozalek, K.L., Durkin, M.M., Lakhlani, P.P., Bonini, J.A., Pathirana, S., Boyle, N., Pu, X., Kouranova, E., Lichtblau, H., Ochoa, F.Y., Branchek, T.A., Gerald, C., 2001. Trace amines: identification of a family of *Mammalian* G protein-coupled receptors. Proc. Natl. Acad. Sci. U. S. A 98, 8966–8971. https://doi.org/10.1073/pnas.151105198.

Bunzow, J.R., Sonders, M.S., Arttamangkul, S., Harrison, L.M., Zhang, G., Quigley, D.I., Darland, T., Suchland, K.L., Pasumamula, S., Kennedy, J.L., Olson, S.B., Magenis, R.E., Amara, S.G., Grandy, D.K., 2001. Amphetamine, 3,4-methylenedioxymethamphetamine, lysergic acid diethylamide, and metabolites of the catecholamine neurotransmitters are agonists of a rat trace amine receptor. Mol. Pharmacol. 60, 1181–1188. https://doi.org/10.1124/mol.60.6.1181.

Cole, S.H., Carney, G.E., McClung, C.A., Willard, S.S., Taylor, B.J., Hirsh, J., 2005. Two functional but noncomplementing *Drosophila tyrosine* decarboxylase genes: distinct roles for neural tyramine and octopamine in female fertility. J. Biol. Chem. 280, 14948–14955. https://doi.org/10.1074/jbc.M414197200.

Davis, M.M., O'Keefe, S.L., Primrose, D.A., Hodgetts, R.B., 2007. A neuropeptide hormone cascade controls the precise onset of post-eclosion cuticular tanning in *Drosophila melanogaster*. Development 134, 4395–4404. https://doi.org/10.1242/dev.009902.

Davis, M.M., Primrose, D.A., Hodgetts, R.B., 2008. A member of the p38 mitogen-activated protein kinase family is responsible for transcriptional induction of dopa decarboxylase in the epidermis of *Drosophila melanogaster* during the innate immune response. Mol. Cell Biol. 28, 4883–4895. https://doi.org/10.1128/mcb.02074-07.

De Luca, M., Roshina, N.V., Geiger-Thornsberry, G.L., Lyman, R.F., Pasyukova, E.G., Mackay, T.F., 2003. Dopa decarboxylase (Ddc) affects variation in *Drosophila longevity*. Nat. Genet. 34, 429–433. https://doi.org/10.1038/ng1218.

Futahashi, R., Fujiwara, H., 2005. Melanin-synthesis enzymes coregulate stage-specific larval cuticular markings in the swallowtail butterfly. *Papilio xuthus*. Dev. Genes Evol. 215, 519–529. https://doi.org/10.1007/s00427-005-0014-y.

Han, Q., Ding, H., Robinson, H., Christensen, B.M., Li, J., 2010. Crystal structure and substrate specificity of *Drosophila* 3,4-dihydroxyphenylalanine decarboxylase. PLoS One 5, e8826. https://doi.org/10.1371/journal.pone.0008826.

Hiruma, K., Riddiford, L.M., 1984. Regulation of melanization of tobacco hornworm larval cuticle *in vitro*. J. Exp. Zool. 230, 393–403. https://doi.org/10.1002/jez.1402300308.

Hiruma, K., Riddiford, L.M., Hopkins, T.L., Morgan, T.D., 1985. Roles of dopa decarboxylase and phenoloxidase in the melanization of the tobacco hornworm and their control by 20-hydroxyecdysone. J. Comp. Physiol. B 155, 659–669. https://doi.org/10.1007/bf00694579.

Huang, C.Y., Chou, S.Y., Bartholomay, L.C., Christensen, B.M., Chen, C.C., 2005. The use of gene silencing to study the role of dopa decarboxylase in mosquito melanization reactions. Insect Mol. Biol. 14, 237–244. https://doi.org/10.1111/j.1365-2583.2004.00552.x.

Jones, D.T., Taylor, W.R., Thornton, J.M., 1992. The rapid generation of mutation data matrices from protein sequences. Comput. Appl. Biosci. 8, 275–282. https://doi.org/10.1093/bioinformatics/8.3.275.

Kumar, S., Stecher, G., Tamura, K., 2016. MEGA7: molecular evolutionary genetics analysis version 7.0 for bigger datasets. Mol. Biol. Evol. 33, 1870–1874. https://doi.org/10.1093/molbev/msw054.

Liu, J., Lemonds, T.R., Popadic, A., 2014. The genetic control of aposematic black pigmentation in hemimetabolous insects: insights from *Oncopeltus fasciatus*. Evol. Dev. 16, 270–277. https://doi.org/10.1111/ede.12090.

Livak, K.J., Schmittgen, T.D., 2001. Analysis of relative gene expression data using real-time quantitative PCR and the 2(-Delta Delta C(T)) Method. Methods 25, 402–408. https://doi.org/10.1006/meth.2001.1262.

Macey, T.A., Liu, Y., Gurevich, V.V., Neve, K.A., 2005. Dopamine D1 receptor interaction with arrestin3 in neostriatal neurons. J. Neurochem. 93, 128–134. https://doi.org/10.1111/j.1471-4159.2004.02998.x.

Majerowicz, D., Alves-Bezerra, M., Logullo, R., Fonseca-de-Souza, A.L., Meyer-Fernandes, J.R., Braz, G.R., Gondim, K.C., 2011. Looking for reference genes for real-time quantitative PCR experiments in *Rhodnius prolixus* (*Hemiptera: Reduviidae*). Insect Mol. Biol. 20, 713–722. https://doi.org/10.1111/j.1365-2583.2011.01101.x.

Mesquita, R.D., Vionette-Amaral, R.J., Lowenberger, C., Rivera-Pomar, R., Monteiro, F.A., Minx, P., Spieth, J., Carvalho, A.B., Panzera, F., Lawson, D., Torres, A.Q., Ribeiro, J.M., Sorgine, M.H., Waterhouse, R.M., Montague, M.J., Abad-Franch, F., Alves-Bezerra, M., Amaral, L.R., Araujo, H.M., Araujo, R.N., Aravind, L., Atella, G.C., Azambuja, P., Berni, M., Bittencourt-Cunha, P.R., Braz, G.R., Calderon-Fernandez, G., Carareto, C.M., Christensen, M.B., Costa, I.R., Costa, S.G., Dansa, M., Daumas-Filho, C.R., De-Paula, I.F., Dias, F.A., Dimopoulos, G., Emrich, S.J., Esponda-Behrens, N., Fampa, P., Fernandez-Medina, R.D., da Fonseca, R.N., Fontenele, M., Fronick, C., Fulton, L.A., Gandara, A.C., Garcia, E.S., Genta, F.A., Giraldo-Calderon, G.I., Gomes, B., Gondim, K.C., Granzotto, A., Guarneri, A.A., Guigo, R., Harry, M., Hughes, D.S., Jablonka, W., Jacquin-Joly, E., Juarez, M.P., Koerich, L.B., Lange, A.B., Latorre-Estivalis, J.M., Lavore, A., Lawrence, G.G., Lazoski, C., Lazzari, C.R., Lopes, R.R., Lorenzo, M.G., Lugon, M.D., Majerowicz, D., Marcet, P.L., Mariotti, M., Masuda, H., Megy, K., Melo, A.C., Missirlis, F., Mota, T., Noriega, F.G., Nouzova, M., Nunes, R.D., Oliveira, R.L., Oliveira-Silveira, G., Ons, S., Orchard, I., Pagola, L., Paiva-Silva, G.O., Pascual, A., Pavan, M.G., Pedrini, N., Peixoto, A.A., Pereira, M.H., Pike, A., Polycarpo, C., Prosdocimi, F., Ribeiro-Rodrigues, R., Robertson, H.M., Salerno, A.P., Salmon, D., Santesmasses, D., Schama, R., Seabra-Junior, E.S., Silva-Cardoso, L., Silva-Neto, M.A., Souza-Gomes, M., Sterkel, M., Taracena, M.L., Tojo, M., Tu, Z.J.,

Tubio, J.M., Ursic-Bedoya, R., Venancio, T.M., Walter-Nuno, A.B., Wilson, D., Warren, W.C., Wilson, R.K., Huebner, E., Dotson, E.M., Oliveira, P.L., 2015. Genome of *Rhodnius prolixus*, an insect vector of Chagas disease, reveals unique adaptations to hematophagy and parasite infection. Proc. Natl. Acad. Sci. U. S. A 112, 14936–14941. https://doi.org/10.1073/pnas.1506226112.

Morgan, B.A., Johnson, W.A., Hirsh, J., 1986. Regulated splicing produces different forms of dopa decarboxylase in the central nervous system and hypoderm of *Drosophila melanogaster*. EMBO J. 5, 3335–3342. https://doi.org/10.1002/j.1460-2075.1986.tb04648.x.

Mun, S., Noh, M.Y., Dittmer, N.T., Muthukrishnan, S., Kramer, K.J., Kanost, M.R., Arakane, Y., 2015. Cuticular protein with a low complexity sequence becomes cross-linked during insect cuticle sclerotization and is required for the adult molt. Sci. Rep. 5, 10484. https://doi.org/10.1038/srep10484.

Nappi, A.J., Carton, Y., Vass, E., 1992. Reduced cellular immune competence of a temperature-sensitive dopa decarboxylase mutant strain of *Drosophila melanogaster* against the parasite *Leptopilina boulardi*. Comp. Biochem. Physiol. B 101, 453–460. https://doi.org/10.1016/0305-0491(92)90027-o.

Paim, R.M., Pereira, M.H., Di Ponzio, R., Rodrigues, J.O., Guarneri, A.A., Gontijo, N.F., Araujo, R.N., 2012. Validation of reference genes for expression analysis in the salivary gland and the intestine of *Rhodnius prolixus* (*Hemiptera, Reduviidae*) under different experimental conditions by quantitative real-time PCR. BMC Res. Notes 5, 128. https://doi.org/10.1186/1756-0500-5-128.

Paskewitz, S.M., Andreev, O., 2008. Silencing the genes for dopa decarboxylase or dopachrome conversion enzyme reduces melanization of foreign targets in *Anopheles gambiae*. Comp. Biochem. Physiol. B Biochem. Mol. Biol. 150, 403–408. https://doi.org/10.1016/j.cbpb.2008.04.010.

Pedrini, N., Mijailovsky, S.J., Girotti, J.R., Stariolo, R., Cardozo, R.M., Gentile, A., Juarez, M.P., 2009. Control of pyrethroid-resistant Chagas disease vectors with entomopathogenic fungi. PLoS Neglected Trop. Dis. 3 e434. https://doi.org/10.1371/journal.pntd.0000434.

Ribeiro, J.M., Genta, F.A., Sorgine, M.H., Logullo, R., Mesquita, R.D., Paiva-Silva, G.O., Majerowicz, D., Medeiros, M., Koerich, L., Terra, W.R., Ferreira, C., Pimentel, A.C., Bisch, P.M., Leite, D.C., Diniz, M.M., Da Silva, M.L., Araujo, R.N., Gandara, A.C., Brosson, S., Salmon, D., Bousbata, S., Gonzalez-Caballero, N., Silber, A.M., Alves-Bezerra, M., Gondim, K.C., Silva-Neto, M.A., Atella, G.C., Araujo, H., Dias, F.A., Polycarpo, C., Vionette-Amaral, R.J., Fampa, P., Melo, A.C., Tanaka, A.S., Balczun, C., Oliveira, J.H., Goncalves, R.L., Lazoski, C., Rivera-Pomar, R., Diambra, L., Schaub, G.A., Garcia, E.S., Azambuja, P., Braz, G.R., Oliveira, P.L., 2014. An insight into the transcriptome of the digestive tract of the bloodsucking bug, *Rhodnius prolixus*. PLoS Neglected Trop. Dis. 8, e2594. https://doi.org/10.1371/journal.pntd.0002594.

Riedel, F., Vorkel, D., Eaton, S., 2011. Megalin-dependent yellow endocytosis restricts melanization in the *Drosophila cuticle*. Development 138, 149–158. https://doi.org/10.1242/dev.056309.

Rowland, I.J., Goodman, W.G., 2016. Magnetic resonance imaging of alimentary tract development in *Manduca sexta*. PLoS One 11, e0157124. https://doi.org/10.1371/journal.pone.0157124.

Sanchez-Jimenez, F., Pino-Angeles, A., Rodriguez-Lopez, R., Morales, M., Urdiales, J.L., 2016. Structural and functional analogies and differences between histidine decarboxylase and aromatic l-amino acid decarboxylase molecular networks: biomedical implications. Pharmacol. Res. 114, 90–102. https://doi.org/10.1016/j.phrs.2016.08.032.

Schaub, G.A., Kleffmann, T., Kollien, A.H., Schmidt, J., 1998. Hydrophobic attachment of *Trypanosoma cruzi* to the rectal cuticle of *Triatoma infestans* and its influence on metacyclogenesis - a review. Tokai J. Exp. Clin. Med. 23, 321–327. https://doi.org/10.1007/s004360050443.

Sideri, M., Tsakas, S., Markoutsa, E., Lampropoulou, M., Marmaras, V.J., 2008. Innate immunity in insects: surface-associated dopa decarboxylase-dependent pathways regulate phagocytosis, nodulation and melanization in medfly haemocytes. Immunology 123, 528–537. https://doi.org/10.1111/j.1365-2567.2007.02722.x.

Sterkel, M., Oliveira, J.H.M., Bottino-Rojas, V., Paiva-Silva, G.O., Oliveira, P.L., 2017. The dose makes the poison: nutritional overload determines the life traits of blood-feeding arthropods. Trends Parasitol. 33, 633–644. https://doi.org/10.1016/j.pt.2017.04.008.

Sterkel, M., Oliveira, P.L., 2017. Developmental roles of tyrosine metabolism enzymes in the blood-sucking insect *Rhodnius prolixus*. Proc. Biol. Sci. 284, 20162607. https://doi.org/10.1098/rspb.2016.2607.

Sterkel, M., Perdomo, H.D., Guizzo, M.G., Barletta, A.B., Nunes, R.D., Dias, F.A., Sorgine, M.H., Oliveira, P.L., 2016. Tyrosine detoxification is an essential trait in the life history of blood-feeding arthropods. Curr. Biol. 26, 2188–2193. https://doi.org/10.1016/j.cub.2016.06.025.

Vavricka, C., Han, Q., Huang, Y., Erickson, S.M., Harich, K., Christensen, B.M., Li, J., 2011. From L-dopa to dihydroxyphenylacetaldehyde: a toxic biochemical pathway plays a vital physiological function in insects. PLoS One 6, e16124. https://doi.org/10.1371/journal.pone.0016124.

Vavricka, C.J., Han, Q., Mehere, P., Ding, H., Christensen, B.M., Li, J., 2014. Tyrosine metabolic enzymes from insects and mammals: a comparative perspective. Insect Sci. 21, 13–19. https://doi.org/10.1111/1744-7917.12038.

Verlinden, H., 2018. Dopamine signalling in locusts and other insects. Insect Biochem. Mol. Biol. 97, 40–52. https://doi.org/10.1016/j.ibmb.2018.04.005.

Wittkopp, P.J., Beldade, P., 2009. Development and evolution of insect pigmentation: genetic mechanisms and the potential consequences of pleiotropy. Semin. Cell Dev. Biol. 20, 65–71. https://doi.org/10.1016/j.semcdb.2008.10.002.

World Health Organization, 2018. WHO Chagas disease (American trypanosomiasis). http://www.who.int/chagas/en/.

Wragg, R.T., Hapiak, V., Miller, S.B., Harris, G.P., Gray, J., Komuniecki, P.R., Komuniecki, R.W., 2007. Tyramine and octopamine independently inhibit serotonin-stimulated aversive behaviors in *Caenorhabditis elegans* through two novel amine receptors. J. Neurosci. 27, 13402–13412. https://doi.org/10.1523/jneurosci.3495-07.2007.